ADVANCED MATERIALS
www.advmat.de

Materials Views
www.MaterialsViews.com

Routing of Deep-Subwavelength Optical Beams and Images without Reflection and Diffraction Using Infinitely Anisotropic Metamaterials

Peter B. Catrysse and Shanhui Fan*

Media that are described by extreme electromagnetic parameters, such as very large or very small permittivity or permeability, have generated significant basic physics interest and applications in recent years. Notable examples include epsilon-near-zero materials,[1,2] ultralow-refractive-index materials,[3] and ultrahigh-refractive-index materials.[4–7] Many photonic structures, including waveguides, lenses, and photonic bandgap materials, benefit greatly from the large index contrast provided by such media.[8,9]

In this paper we discuss media with infinite anisotropy, by which we mean that the permittivity (permeability) is infinite in one direction and finite in the other directions. As a specific case, we consider a uniaxial anisotropic medium with a permittivity tensor:

$$\bar{\bar{\varepsilon}} = \varepsilon_0 \begin{pmatrix} \varepsilon_\perp & 0 & 0 \\ 0 & \varepsilon_\perp & 0 \\ 0 & 0 & \varepsilon_z \end{pmatrix} \quad (1)$$

where ε_0 is the permittivity of vacuum, while $\varepsilon_\perp$ and ε_z are the (relative) transverse and longitudinal permittivities. If $\varepsilon_z \to \infty$ and $\varepsilon_\perp$ is finite, the medium is infinitely anisotropic. We use an infinitely anisotropic permittivity tensor to control transverse magnetic (TM) polarization. The control of transverse electric polarization using an infinitely anisotropic permeability tensor can be developed in a similar fashion. Previously, we showed efficient light transport in deep-subwavelength apertures filled with infinitely anisotropic media for both polarizations.[10] Here, we point out some of the opportunities that exist for controlling light at the nanoscale using infinitely anisotropic media by themselves. While diffraction-free propagation of deep-subwavelength beams and images has been shown,[11–13] we demonstrate in this work that the interfaces between two infinitely anisotropic media with different orientations enable complete deep-subwavelength beams to bend sharply (with zero bend radius) and without any reflections. This unusual behavior opens up new possibilities for routing of deep-subwavelength beams and images.

The paper is organized as follows. Firstly, we show numerically reflectionless, diffraction-free routing of a deep-subwavelength beam and shadow using first-principles electromagnetic-field simulations based on a finite-difference time-domain (FDTD) method.[14] Next, we account for this remarkable behavior analytically. Finally, we demonstrate how to achieve an infinite anisotropy using a metamaterial design that can be implemented with existing materials over a substantial bandwidth.

In our numerical simulations, we consider TM polarization (E_x, H_y, E_z) for two media with infinite anisotropy, medium 1 with $\varepsilon_\perp = 4$ and $\varepsilon_z = 1 \times 10^{10}$ (approximating $\varepsilon_z \to \infty$) and medium 2 with $\varepsilon_\perp = 4$ and $\varepsilon_x = 1 \times 10^{10}$, which form a 45° interface. The propagation is in the z-direction ($\perp$ defines the transverse xy-plane) in the first medium and it is in the x-direction ($\perp$ defines the transverse yz-plane) in the second medium. **Figure 1** shows the magnetic field $|H_y|$ for a deep-subwavelength

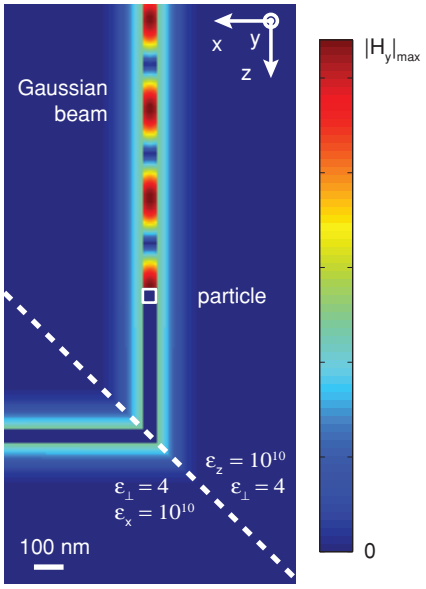

Figure 1. Reflectionless, diffraction-free routing with zero bend radius of a deep-subwavelength beam and shadow at the interface between two media with infinite anisotropy. $|H_y|$ is shown for a transverse magnetically polarized (E_x, H_y, E_z) beam propagating vertically down (+z-direction) and bending 90° left (+x-direction) at a 45° media interface (dashed white line). The fields are obtained with an exact finite-difference time-domain (FDTD) method for a uniaxial anisotropic medium with $\varepsilon_z = 1 \times 10^{10}$, $\varepsilon_\perp = 4$ (above the dashed white line) and one with $\varepsilon_x = 1 \times 10^{10}$, $\varepsilon_\perp = 4$ (below the dashed white line). The shadow results from a 50 nm-wide perfect electrical conductor (PEC) particle with square cross-section (represented by the white outline) which is illuminated by the beam from the top.

Dr. P. B. Catrysse, Prof. S. Fan
E. L. Ginzton Laboratory and Department of Electrical Engineering
Stanford University
Stanford, California 94305, USA
E-mail: pcatryss@stanford.edu

DOI: 10.1002/adma.201203528

beam with a wavelength $\lambda = 1.55$ μm when it is incident from medium 1 (above the dashed white line) onto medium 2 (below the dashed white line). The beam has a Gaussian transverse profile (150 nm full-width half-maximum), propagates from top to bottom (+*z*-direction) in medium 1, illuminates a 50 nm-wide, perfect electrical conductor (PEC) particle with square cross-section (represented by the white outline), and forms a perfect shadow behind the particle. When the beam and the shadow encounter the interface (dashed white line), they both make a sharp 90° bend to the left (+*x*-direction) with zero bend radius and without any reflections.

Figure 1 demonstrates unambiguously that an interface between two infinitely anisotropic media allows for reflectionless, diffraction-free routing of complete deep-subwavelength beams and shadows. We note that the particle reflects the central part of the beam while allowing the tails of the beam to propagate unperturbed. As a result, we see a strong standing-wave pattern for the central part of the transverse field profile in front of the particle and a perfect shadow in the center of the transverse field profile behind the particle. The standing-wave pattern and the shadow are each 50 nm wide and they are defined with geometrical precision. There are no diffraction effects during propagation and transmission at the interface observed in Figure 1 despite the deep-subwavelength dimensions of the beam ($<\lambda/10$) and the shadow ($<\lambda/30$).

We now account for these numerical results analytically and describe the electromagnetic properties of interfaces between two media with infinite anisotropy that give rise to them. Firstly, we provide a brief discussion of beam propagation in a single medium with infinite anisotropy.

Diffraction-Free Propagation of a Deep-Subwavelength Beam and Shadow With Arbitrary Shape: For a wave $E(\mathrm{r}) = E_0 \exp(i\,\mathrm{k}\cdot\mathrm{r})$ propagating in a uniaxial anisotropic medium with permittivity tensor $\bar{\bar{\varepsilon}}$, given by Equation 1, we have $|\mathrm{k}|^2 = k^2{}_z + k_\perp{}^2$ and $\omega^2/c^2 = k_z^2/\varepsilon_\perp + k_\perp^2/\varepsilon_z$ (the latter describes a constant frequency contour for fixed ω). k_z and $k_\perp$ are the longitudinal (propagation in *z*-direction) and transverse (*xy*-plane) wave vector components, respectively. k_z needs to be real for propagating waves. In the case of infinite anisotropy ($\varepsilon_z \to \infty$), this becomes:

$$\frac{\omega^2}{c^2} = \frac{k_z^2}{\varepsilon_\perp} \tag{2}$$

Equation 2 is independent of $k_\perp$ (i.e., propagating waves can take on any $k_\perp$ value). Such a medium does not limit transverse wave vectors and, hence, supports deep-subwavelength beams. Equation 2 also implies that waves with different $k_\perp$ propagate with the same k_z (i.e., they accumulate the same phase upon propagation over a distance *z*), which prevents beam diffraction. The propagation velocity meanwhile is controlled by the transverse permittivity $\varepsilon_\perp$ and is nonzero. An infinitely anisotropic medium ($\varepsilon_z \to \infty$) therefore allows diffraction-free propagation with finite velocity for beams of arbitrary shape and size. It is important to realize that Equation 2 refers to fully three-dimensional beam propagation since $k_\perp$ refers to transverse wave vector components in the full transverse *xy*-plane. Wave vector components are not limited by the medium in both transverse dimensions and propagate with the same k_z for a given frequency. Hence, this medium allows for diffraction-free propagation of three-dimensional beams with deep-subwavelength confinement in both transverse dimensions.

One interesting property of a medium with infinite anisotropy, as pointed out by Catrysse and Fan,[10] is that all modes propagating inside the medium are purely transverse electromagnetic (TEM) modes. For TM polarization, we have in general (E_x, H_y, E_z). The magnetic field is always transverse along the *y* direction. The Poynting vector of each $k_\perp$ is always in the *z* direction; therefore, we must have $E_z = 0$. Hence, all waves in this medium are truly TEM waves with $\left(E_0, \sqrt{\varepsilon_\perp}E_0, 0\right)$. We also observe that the impedance matching necessary to couple into this medium from the outside involves transverse permittivity only. Since $\varepsilon_\perp$ is finite, it can be matched to the surrounding medium so that no reflections occur at the interface.[10]

Reflectionless Routing or Manipulation of a Deep-Subwavelength Beam: We consider now two media with infinite anisotropy (i.e., $\varepsilon_{z1} \to \infty$ in a first medium and $\varepsilon_{z2} \to \infty$ in a second medium), and assume further that z_1 and z_2 are not coaligned (**Figure 2**a). The propagation in each individual medium is along z_1 and z_2 only, and the in-plane electric fields are fixed along $\perp_1$ and $\perp_2$, respectively. We consider that directions z_1 and z_2 make angles θ_1 and θ_2 with the interface. In a common co-ordinate system with the $\perp$-axis defined parallel to the interface, the wave fields are $\left(E_0\cos\theta_1,\ E_0\sqrt{\varepsilon_{\perp 1}},\ -E_0\sin\theta_1\right)$ and $\left(E_0\cos\theta_2,\ E_0\sqrt{\varepsilon_{\perp 2}},\ -E_0\sin\theta_2\right)$, where $\varepsilon_{\perp 1}$ and $\varepsilon_{\perp 2}$ are the transverse permittivities in the respective media. It is easily verified that the wave impedance (E_x/H_y) in each medium is the same when:

$$\sqrt{\varepsilon_{\perp 1}}\cos\theta_2 = \sqrt{\varepsilon_{\perp 2}}\cos\theta_1 \tag{3}$$

As soon as Equation 3 is satisfied, the two media are impedance-matched and there are no reflections at the interface. Since the direction of propagation and the fields are pinned down inside each medium, this applies to any plane wave irrespective of its transverse wave vector. By extension, it also applies to any collection of waves with arbitrary transverse wave vectors. Any beam is therefore also perfectly impedance-matched when Equation 3 holds, and passes through the interface without reflections. While a reflectionless interface has been noted before between two conventional anisotropic media,[15] our original contribution here consists of demonstrating that interfaces between infinitely anisotropic media allow for reflectionless routing of completely diffraction-free deep-subwavelength beams and images. By choosing $\varepsilon_{\perp 1} = \varepsilon_{\perp 2}$ and $\theta_1 = -\theta_2 = 45°$, for example, we create an impedance-matched interface for deep-subwavelength beams that supports 90° zero-radius bending and thus sharp routing of such beams without any reflections. We note that Equation 3 is very general and provides a condition that allows for zero-radius bending of deep-subwavelength beams at any arbitrary angle.

We now calculate the transmission and reflection at the interface between these two media for an arbitrary set of principal-axis orientations (i.e., for an arbitrary set of θ_1 and θ_2). By applying conservation of the parallel wave vectors and enforcing the continuity of the tangential electric and magnetic fields, we obtain the following exact analytic expressions for the transmittance and reflectance:

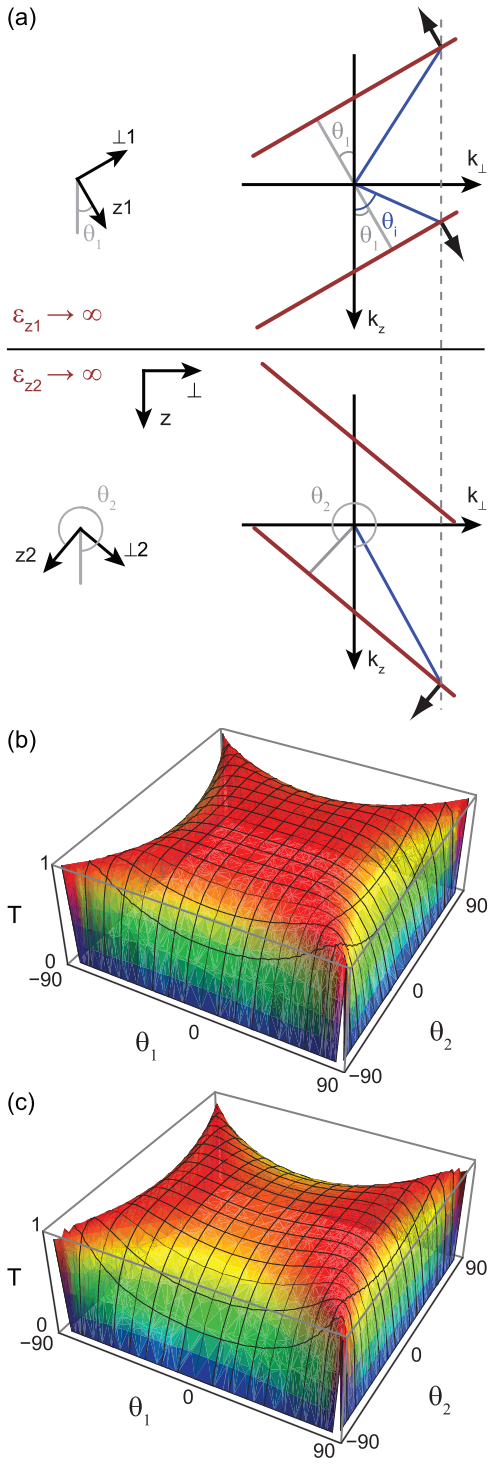

Figure 2. a) Interface between two media with infinite anisotropy along different directions. The directions z_1 in medium 1 ($\varepsilon_{z1} \to \infty$, top) and z_2 in medium 2 ($\varepsilon_{z2} \to \infty$, bottom) make angles θ_1 and θ_2 with the interface. The geometry and angles are shown on the left-hand side. The constant frequency contour diagrams in the respective media are shown on the right-hand side (medium 1 at the top and medium 2 at the bottom). b,c) Transmittance at an interface between two media with infinite anisotropy along different directions. The transmittance for any combination of θ_1 and θ_2 ranging from −90° to 90° is shown. The respective media have: b) $\varepsilon_{z1} \to \infty$, $\varepsilon_{\perp 1} = 4$ and $\varepsilon_{z2} \to \infty$, $\varepsilon_{\perp 2} = 4$, and c) $\varepsilon_{z1} \to \infty$, $\varepsilon_{\perp 1} = 4$ and $\varepsilon_{z2} \to \infty$, $\varepsilon_{\perp 2} = 12$.

$$T = \frac{4\sqrt{\varepsilon_{\perp 1}\varepsilon_{\perp 2}}\cos\theta_1\cos\theta_2}{\left(\sqrt{\varepsilon_{\perp 1}}\cos\theta_2 + \sqrt{\varepsilon_{\perp 2}}\cos\theta_1\right)^2},$$

$$R = \frac{\left(\sqrt{\varepsilon_{\perp 1}}\cos\theta_2 - \sqrt{\varepsilon_{\perp 2}}\cos\theta_1\right)^2}{\left(\sqrt{\varepsilon_{\perp 1}}\cos\theta_2 + \sqrt{\varepsilon_{\perp 2}}\cos\theta_1\right)^2} \quad (4)$$

A detailed derivation of these equations can be found in the Supporting Information.

Equation 4 resembles the Fresnel formulae for an interface between two isotropic dielectric media.[16] Unlike the regular Fresnel formulae, however, θ_1 and θ_2 depend on the orientation of the media with respect to the interface (i.e., the expressions here are independent of the transverse wave vector of the incident beam). The transmittance and reflectance therefore do not vary with the transverse wave vector of the beam once the media orientations are chosen. We conclude from Equation 4 that the interface becomes impedance-matched and transmits without reflections ($T = 1$ and $R = 0$) when $\sqrt{\varepsilon_{\perp 1}}\cos\theta_2 = \sqrt{\varepsilon_{\perp 2}}\cos\theta_1$. This result also confirms the impedance analysis we carried out above.

Figure 2b,c show the transmittance through an interface between two media with infinite anisotropy as a function of the angles θ_1 and θ_2. In Figure 2b, the media are characterized by the same transverse permittivity (i.e., $\varepsilon_{z1} \to \infty$, $\varepsilon_{\perp 1} = 4$ and $\varepsilon_{z2} \to \infty$, $\varepsilon_{\perp 2} = 4$, respectively). Since $\varepsilon_{\perp 1} = \varepsilon_{\perp 2}$ in this case, we observe perfect transmittance when $\theta_2 = \pm\theta_1$. Figure 2c shows the transmittance for an interface between two infinitely anisotropic media with different transverse permittivities ($\varepsilon_{z1} \to \infty$, $\varepsilon_{\perp 1} = 4$ and $\varepsilon_{z2} \to \infty$, $\varepsilon_{\perp 2} = 12$). It confirms that perfect transmission holds very generally for any chosen orientation of the media given that Equation 3 is satisfied. It is important to note that the transmittance maps in Figure 2b,c remain unchanged when the transverse wave vector of the incident wave is changed. These are universal maps for waves (and beams) irrespective of their transverse wave vector.

Design of Metamaterials with Infinite Anisotropy: Simultaneous finite transverse permittivity and infinite longitudinal permittivity are hard to find in naturally occurring materials, but can be achieved with a metamaterial design. For TM polarization, $\varepsilon_z \to \infty$ can be obtained, for instance with a one-dimensional (1D) periodic structure (period a) comprising two alternating layers (in the z-direction) that have positive and negative permittivity, respectively (**Figure 3**a inset).[5,12] When the thickness of each layer is much smaller than the operating wavelength, such a metamaterial homogenizes to an effective medium with:

$$\varepsilon_\perp = f\varepsilon_1 + (1-f)\varepsilon_2,$$

$$\varepsilon_z = \frac{\varepsilon_1\varepsilon_2}{(1-f)\varepsilon_1 + f\varepsilon_2}, \quad (5)$$

where ε_1 (>0) and ε_2 (<0) are the relative permittivities of the layer materials, while f and $1 - f$ are the fractions of the total volume occupied by each layer.[16] In Equation 5, $\varepsilon_z \to \infty$ when $(1 - f)\varepsilon_1 + f\varepsilon_2 = 0$. This system therefore has infinite anisotropy with:

$$\varepsilon_\perp = \varepsilon_1 + \varepsilon_2,$$

$$\varepsilon_z \to \infty \quad (6)$$

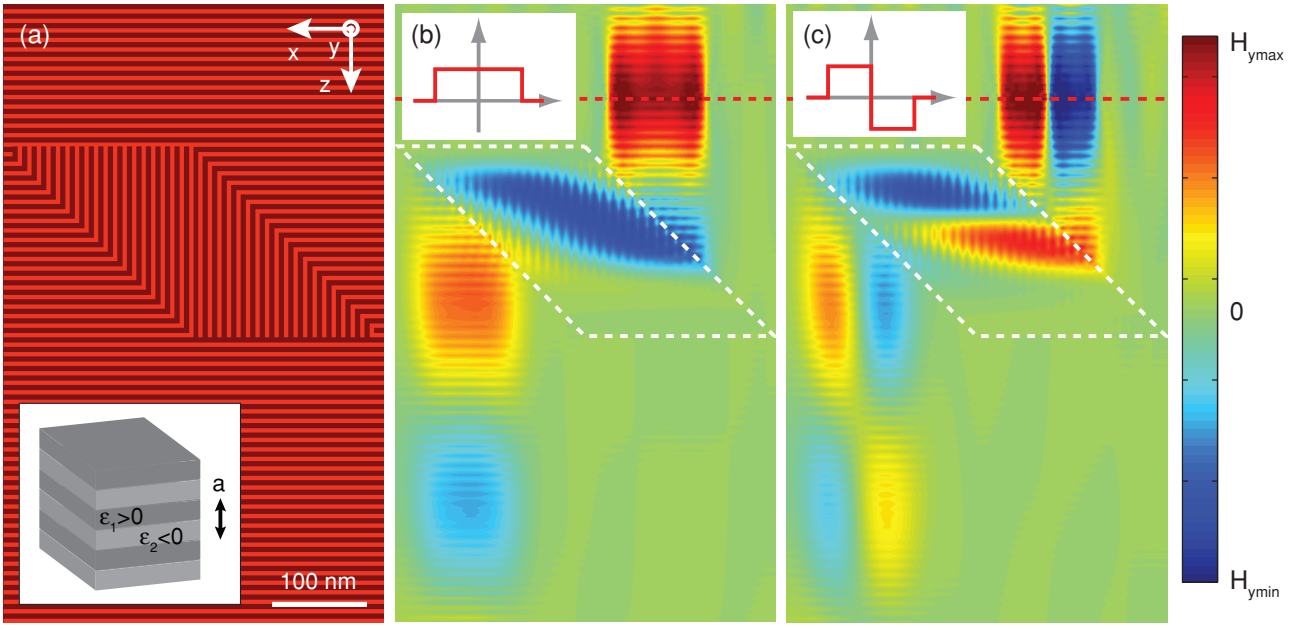

Figure 3. Reflectionless, diffraction-free routing with zero bend radius of deep-subwavelength beams using interfaces between metamaterials with very large anisotropy. a) Interface geometry in which metamaterial 1 (background) consists of horizontal layers, and metamaterial 2 (parallelogram-shaped region) is made up of vertically oriented layers. The inset shows the metamaterial geometry consisting of a 1D periodic structure (period a) and two alternating layers ($\varepsilon_1 > 0$ and $\varepsilon_2 < 0$) in the direction of propagation. b,c) The real part of the magnetic-field distribution for propagating top-hat beams (100 nm wide) with uniform phase across the beam (b) and a π phase shift in the middle of the beam (c). The dashed red line shows the location of each beam excitation.

when $f = \varepsilon_1/(\varepsilon_1 - \varepsilon_2)$ (note that f is a positive value between 0 and 1).

In the Supporting Information, we include further details on how this very large anisotropy is designed over a substantial bandwidth. We also confirm the homogenization argument by band-diagram analysis based on rigorous electromagnetic calculations for periodicities a <20 nm. Here instead, we show a practical design based on existing materials to illustrate that the novel effects we predict can be achieved with standard plasmonic and dielectric materials. Specifically, we demonstrate reflectionless, diffraction-free routing of deep-subwavelength optical beams inside metamaterials designed based on the aforementioned principles. For this demonstration, we employ a finite-difference frequency-domain (FDFD) method to solve Maxwell's equations.[17] This allows us to describe materials using measured permittivities at the operating wavelength (λ = 620 nm), thus directly taking into account material dispersion as well as loss. We define a 45° interface geometry comprising two metamaterials to demonstrate sharp bending and routing with zero bend radius. Each metamaterial consists of a 1D periodic structure with alternating layers of $\varepsilon_1 = 12$ (corresponding to the permittivity of $Al_{0.6}Ga_{0.4}As$ at 620 nm) and $\varepsilon_2 = -10.06 + 0.82i$ (corresponding to the permittivity of Au at 620 nm).[18,19] The volume fractions of these layers are 0.55 and 0.45 for a periodicity a = 10 nm. This metamaterial design achieves $\varepsilon_z > 250$ and $\varepsilon_\perp = 2$ and therefore very large anisotropy. Figure 3a shows the interface geometry. Metamaterial 1 (background) consists of horizontal layers, while metamaterial 2 (region outlined by the parallelogram) is made up of vertically oriented layers. We excite a TM polarized beam inside metamaterial 1 (at dashed red line in Figure 3b,c) with a 100 nm wide transverse top-hat profile and uniform phase (Figure 3b, inset) as well as with a π phase shift in the middle of the beam (Figure 3c, inset). Figure 3b,c show the real part of the magnetic-field distribution for each beam as it propagates. We clearly observe diffraction-free propagation in the vertical z-direction inside metamaterial 1, a reflectionless 90° zero-radius bend at the first 45° interface (dashed white line), diffraction-free propagation in the horizontal x-direction inside metamaterial 2, and a reflectionless 90° zero-radius bend at the second 45° interface (dashed white line).

These numerical results show "ray-like" propagation of deep-subwavelength beams inside a metamaterial with very large anisotropy implemented using existing materials. They also illustrate reflectionless bending of deep-subwavelength beams with zero bend radius at the interface between two realizable metamaterials. In addition, they demonstrate deep-subwavelength routing of beams modulated in amplitude or phase at the nanoscale. Since there is no loss of resolution due to diffraction during beam routing, they also indicate the ability to perform deep-subwavelength imaging using infinitely anisotropic metamaterials with reflectionless interfaces. The novel physics brought forth by the ideal case of infinite anisotropy can therefore be realized in a practical metamaterial design with material loss included. We emphasize that these metamaterials enable deep-subwavelength confinement in both transverse dimensions (i.e., they allow diffraction- and reflection-free control of fully three-dimensional beam propagation).

We have shown that interfaces between two media with infinite anisotropy can be impedance-matched for complete deep-subwavelength beams, that they can enable reflectionless routing with zero bend radius, and that this routing is entirely free from diffraction effects even when deep-subwavelength information is encoded on the beams. These unusual behaviors indicate an unprecedented possibility of using media with infinite anisotropy to manipulate beams with deep-subwavelength features, including complete images. To illustrate physical realizability, we demonstrated these behaviors in a realistic metamaterial design with very large anisotropy. Due to the planar geometry of our design, well-established planar nanofabrication techniques can be used to implement such metamaterials. This should allow for further experimentation. Hence, our approach opens the door to deep-subwavelength routing of information-carrying beams as well as far-field imaging at the deep-subwavelength scale unencumbered by the usual effects of diffraction and reflection.

Experimental Section

Numerical Methods: The numerical experiments in this work were performed using first-principles, full-field electromagnetic calculations. For our demonstrations involving infinitely anisotropic media, we employed an FDTD method.[14] The 2D simulation domain consisted of a rectangular grid with grid size set to 0.5 nm and was terminated by perfectly matched layer (PML) boundaries. Inside the domain, we defined a 45° interface geometry comprising two infinitely anisotropic media (medium 1: $\varepsilon_{\perp} = 4$ and $\varepsilon_z = 1 \times 10^{10}$; medium 2: $\varepsilon_{\perp} = 4$ and $\varepsilon_x = 1 \times 10^{10}$). In all of the FDTD simulations, we assumed a continuous-wave excitation source with wavelength $\lambda = 1.55$ μm. For our numerical demonstrations of a physically realizable metamaterial, we employed an FDFD approach to solve Maxwell's equations.[17] In FDFD, the electromagnetic fields were obtained by solving a large sparse linear system. The simulation domain consisted of a 2D rectangular grid with the grid size set to 0.5 nm and terminated by PML boundaries. Inside the domain, we defined a 45° interface geometry comprising two metamaterials. The metamaterials consisted of a 1D periodic structure with alternating layers of $\varepsilon_1 = 12$ and $\varepsilon_2 = -10.06 + 0.82i$ (volume fractions were 0.55 and 0.45). The periodicity a was 10 nm along the vertical direction for the first metamaterial and 10 nm in the horizontal direction for the second metamaterial. In all of the FDFD simulations, we assumed a wavelength $\lambda = 620$ nm.

Supporting Information

Supporting Information is available from the Wiley Online Library or from the author.

Acknowledgements

This research was supported in part by the Department of Energy, Grant No. DE-FG02-07ER46426.

Received: August 23, 2012
Revised: October 11, 2012
Published online: November 26, 2012

[1] M. Silveirinha, N. Engheta, *Phys. Rev. Lett.* **2006**, *97*, 157403.
[2] B. Edwards, A. Alu, M. E. Young, M. Silveirinha, N. Engheta, *Phys. Rev. Lett.* **2008**, *100*, 033903.
[3] B. T. Schwartz, R. Piestun, *J. Opt. Soc. Am. B* **2003**, *20*, 2448.
[4] J. T. Shen, P. B. Catrysse, S. H. Fan, *Phys. Rev. Lett.* **2005**, *94*, 197401.
[5] J. Shin, J. T. Shen, P. B. Catrysse, S. H. Fan, *IEEE J. Sel. Top. Quantum Electron.* **2006**, *12*, 1116.
[6] J. Shin, J. T. Shen, S. H. Fan, *Phys. Rev. Lett.* **2009**, *102*, 093903.
[7] M. Choi, S. H. Lee, Y. Kim, S. B. Kang, J. Shin, M. H. Kwak, K. Y. Kang, Y. H. Lee, N. Park, B. Min, *Nature* **2011**, *470*, 369.
[8] B. T. Schwartz, R. Piestun, *Appl. Phys. Lett.* **2004**, *85*, 1.
[9] J. Christensen, F. J. G. de Abajo, *Phys. Rev. B* **2010**, *82*, 161103(R).
[10] P. B. Catrysse, S. H. Fan, *Phys. Rev. Lett.* **2011**, *106*, 223902.
[11] P. A. Belov, C. R. Simovski, P. Ikonen, *Phys. Rev. B* **2005**, *71*, 193105.
[12] P. A. Belov, Y. Hao, *Phys. Rev. B* **2006**, *73*, 113110.
[13] S. Han, Y. Xiong, D. Genov, Z. W. Liu, G. Bartal, X. Zhang, *Nano Lett.* **2008**, *8*, 4243.
[14] A. Taflove, S. C. Hagness, *Computational Electrodynamics: the Finite-Difference Time-Domain Method. 2nd ed.*, Artech House, Boston **2000**.
[15] Y. Zhang, B. Fluegel, A. Mascarenhas, *Phys. Rev. Lett.* **2003**, *91*, 157404.
[16] M. Born, E. Wolf, *Principles of Optics: Electromagnetic Theory of Propagation, Interference and Diffraction of Light. 6th (corrected) ed.*, Pergamon Press, Oxford/New York **1980**.
[17] G. Veronis, S. Fan, in *Surface Plasmon Nanophotonics*, (Eds: M. L. Brongersma, P. Kik), Springer, New York **2007**.
[18] D. E. Aspnes, S. M. Kelso, R. A. Logan, R. Bhat, *J. Appl. Phys.* **1986**, *60*, 754.
[19] D. R. Lide, *CRC Handbook of Chemistry and Physics, 90th ed.*, CRC Press, Boca RatonFL, USA **2009**.